# Electronic Supplementary Information for

# Improvement in Photoelectrochemical Water-Splitting Performance Using GaN Nanowires with Bundle Structures

Sangmoon Han, Siyun Noh, Jaehyeok Shin, Yeon-Tae Yu, Cheul-Ro Lee, and Jin Soo Kim*

Department of Electronic and Information Materials Engineering, Division of Advanced Materials Engineering, and Research Center of Advanced Materials Development, Jeonbuk National University, Jeonju 54896, South Korea

*Corresponding author e-mail: kjinsoo@jbnu.ac.kr (J. S. Kim) Tel.: +82-63-270-2291; Fax: +82-63-270-2305

**Three-dimensional field-emission scanning electron microscopy (FE-SEM) images of the photoanodes measured before photoelectrochemical water splitting (PEC-WS) reaction**

Fig. S1 shows the three-dimensional FE-SEM images of the refernce NWs (Ref-NW) and GaN-NW buldles (GNW-BDLs). The surface morphologies of the Ref-NW and GNW-BDL photoanodes were analyzed by the FE-SEM installed in the 'Future Energy Convergence Core Center' at Jeonbuk National University. For the Ref-NW as shown in Fig. S1a, GaN NWs were independently observed without bundle features. However, the bundle structures were clearly observed when the GaN NWs were dipped into accetone. As shown in Fig. S1b-d , the number of GaN NWs constituting the bundle structures increased with increasing dipping time. The spatial densities of the GNW-BDL structures for GNW-B10, GNW-B20, and GNW-B30 were measured to be $2.5 \times 10^9$, $1.6 \times 10^9$, and $1.0 \times 10^9$ $cm^{-2}$, respectively.

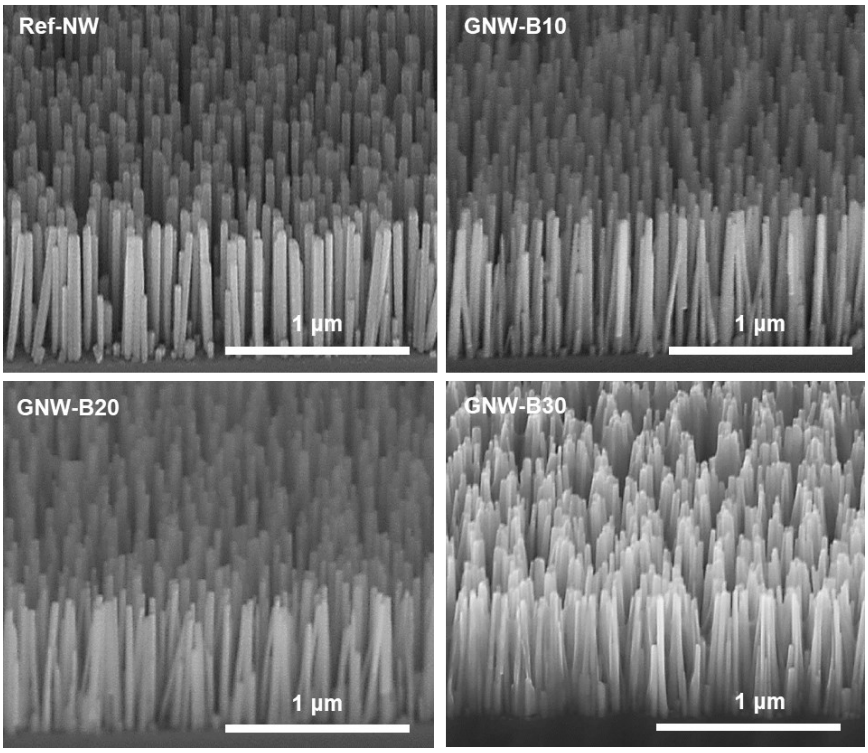


**Fig. S1** Three-dimensional FE-SEM images of the (a) Ref-NW, (b) GNW-B10, (c) GNW-B20, and (d) GNW-B30 photoanodes.

**PEC-WS characteristics of the GNW-B20 photoanode performed in three different electrolytes**

Fig. S2a and b show the current density (*J*)-voltge (*V*) characteristic curves of the GNW-B20 photoanode under dark and illumination conditions in three different electrolytes. In the dark, the current densities of the GNW-B20 photoanodes in the 5-M $H_2SO_4$, 0.5-M NaOH, and 0.5-M KOH electrolytes were measured to be 57.1, 40.3, and 19.1 μA/cm$^2$, respectively. Upon exposure to illumination at the light intensity of 100 mW/cm$^2$, the current densities of the GNW-B20 photoanodes in 5-M $H_2SO_4$, 0.5-M NaOH, and 0.5-M KOH were measured to be 2.2, 1.4, and 1.1 mA/cm$^2$, respectively, at the potential of 0.6 V vs reversible hydrogen electrode (RHE). Fig. S2c shows the applied bias photon-to-current efficiency (ABPE) of the Ref-NW and GNW-BDL photoanodes calculated from the *J-V* characteristic curves. The maximum ABPEs of the Ref-NW, GNW-B10, GNW-B20, and GNW-B30 photoanodes were calculated to be 1.9, 1.5, and 1.5%, respectively. The PEC-WS performances in 0.5-M $H_2SO_4$ was higher than those of other electrolytes, which is consistent with previoursly reported result on the GaN-based photoanodes.[1] Fig. S2d shows the time-dependent current density of the GNW-B20 photoanode measured in three different electrolytes at 0.6 vs RHE. After six hours of PEC-WS operation, the current densities of the GNW-B20 photoanode in the 0.5-M $H_2SO_4$, 0.5-M NaOH, and 0.5-M KOH electrolytes were measured to be 1.62, 0.53, and 0.06 mA/cm$^2$, respectively, which are equivalent to 73.6, 37.5, and 5.4% of those obtained immediately after the reaction. This result indicates that the GNW-B20 photoanode in 0.5-M $H_2SO_4$ is more stable than the other electrolytes.

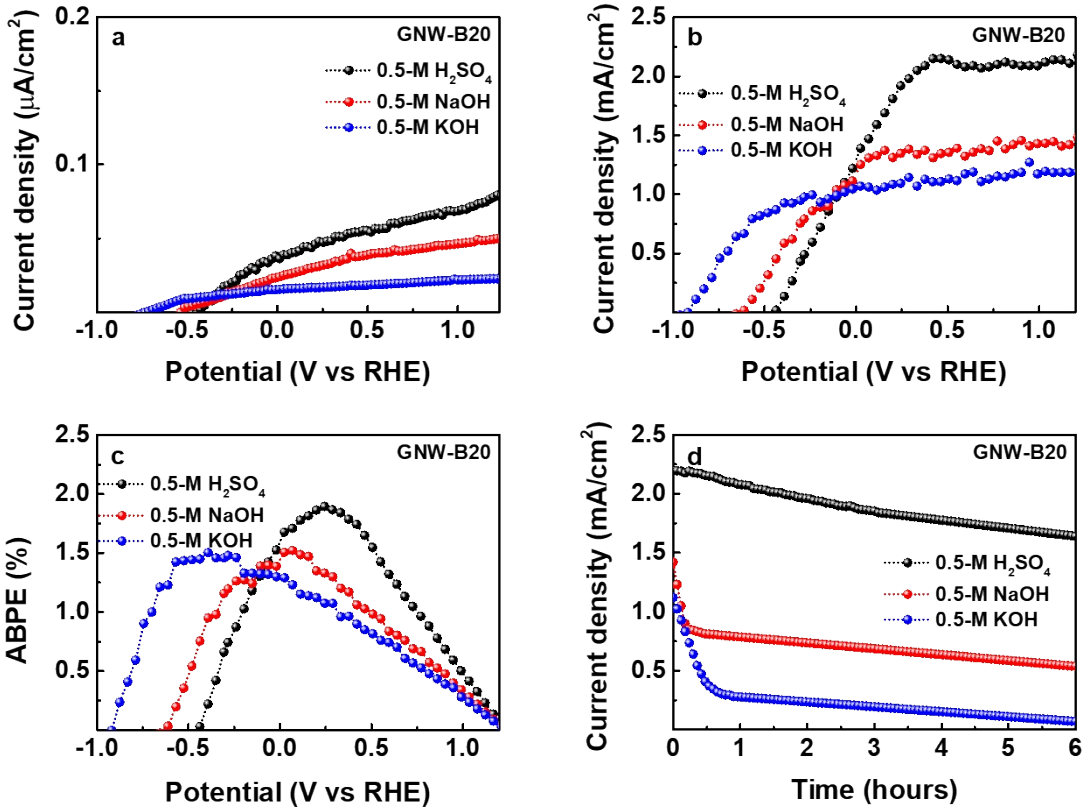


**Fig. S2** *J-V* characteristic curves of the GNW-B20 photoanode (a) in the dark and (b) when illuminated in the 0.5-M $H_2SO_4$, 0.5-M NaOH, and 0.5-M KOH electrolytes. (c) ABPEs calculated from the *J-V* characteristic curves and (d) the current density as a function of time.

**Absorption and transmittance spectra of the Ref-NW and GNW-BDL photoanodes**

Around the wavelength of 360 nm corresponding to energy band-gap of the GaN NWs, the maximum absorbance was observed in the absorption spectra of the photoanodes, and then drastically decreased with increasing the wavelength. On the other hand, the transmittance spectra show the significant increase above the band-gap wavelength. The absorption and transmittance spectra depending on the wavelength are well consistent with IPCE results, indicating that the incident light on the photoanodes effectively contributed to the generation of carriers.

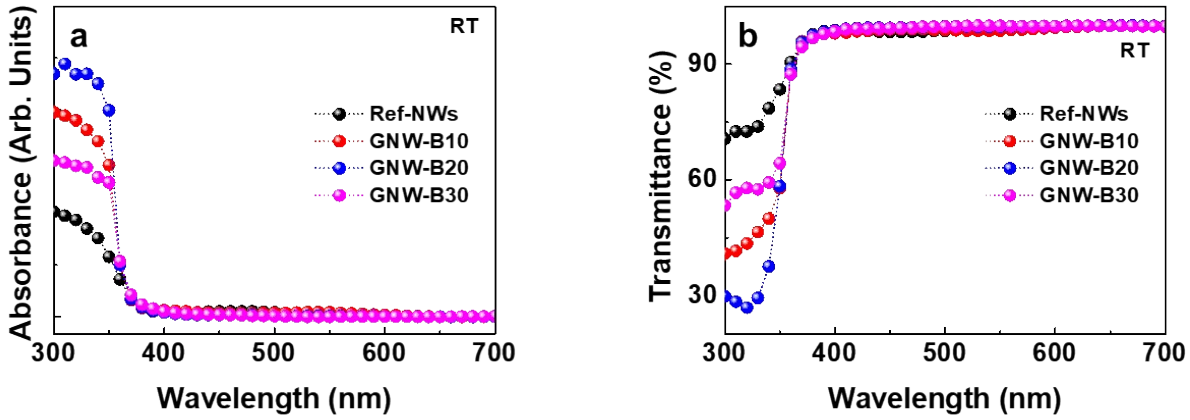


**Fig. S3** (a) Absorption and (b) transmittance spectra of the Ref-NW and GNW-BDL photoanodes.

**The amount of ideal hydrogen and oxygen gases for the Ref-NW and GNW-BDL photoanodes.**

Fig. S4a and b show the amount of ideal hydrogen and oxygen gases calculated from the current densities of the Ref-NW and GNW-BDL photoanodes, respectively. After the six-hour PEC-WS operation, the total amount of hydrogen (oxygen) gas for the Ref-NW, GNW-B10, GNW-B20, and GNW-B30 was measured to be 55.6 (25.8), 105.1 (48.8), 179.2 (83.4), and 141.6 μmol/cm$^2$ (66.8 μmol/cm$^2$), respectively.

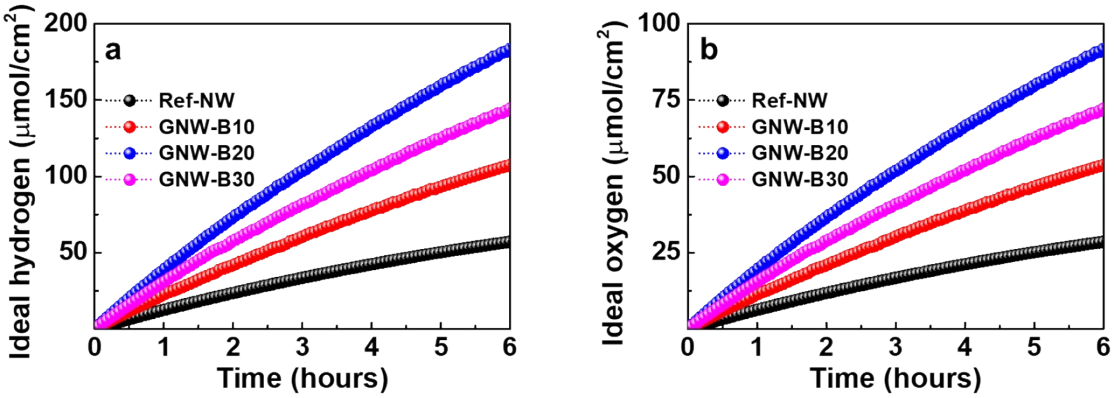


**Fig. S4** The amount of (a) hydrogen and (b) oxygen gases for the Ref-NW and GNW-BDL photoanodes during six-hour PEC-WS operation.

**PEC-WS performance of the GNW-B20 photoanode in two-electrode configuration**

Fig. S5a shows the *J-V* characteristic curve of GNW-B20 measured immediately after the PEC-WS reaction in the two-electrode configuration. The current density obtained after six-hour operation is also considered. At the potential of 0 V, the current density was measured to be 0.15 mA/cm$^2$ because of negative onset potential (-0.14 V vs Pt). The time-dependent current density of the GNW-B20 photoanode measured at 0 V vs Pt in the two-electrode configuration is also shown in Fig. S5b. The current density measured after six-hour PEC-WS reaction was measured to be 0.11 mA/cm$^2$, which corresponding to 73% of that (0.15 mA/cm$^2$) obtained immediately after the reaction.

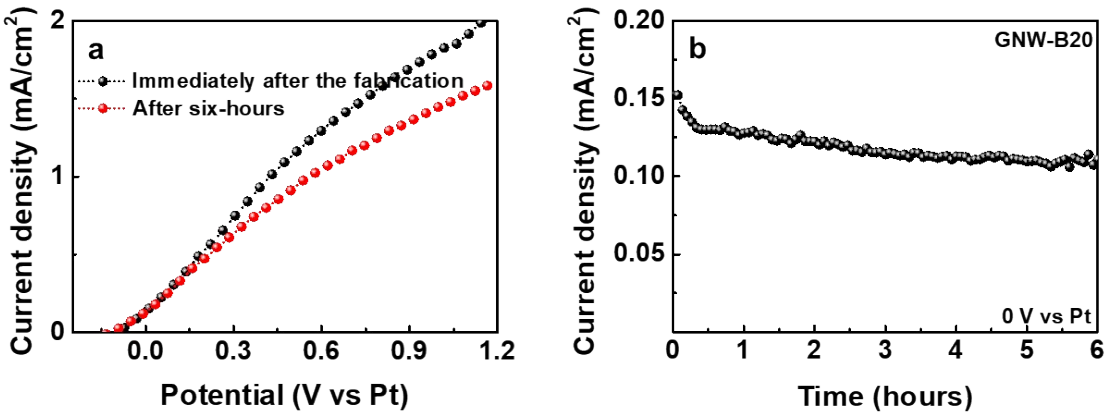


**Fig. S5** (a) *J-V* characteristic curves under illumination and (b) time dependence of the current density of the GNW-B20 photoanode measured at 0 V vs Pt in the two-electrode configuration.

## Notes and references

1 K. Koike, K. Yamamoto, S. Ohara, T. Kikitsu, K. Ozasa, S. Nakamura, M. Sugiyama, Y. Nakano and K. Fujii, *Int. J. Hydrog. Energy* 2017, **15**, 9493-9499.